Noise prediction for serrated trailing-edges

Benshuai Lyu [1] Mahdi Azarpeyvand [2] Samuel Sinayoko [3]

[1]Department of Engineering, University of Cambridge

[2]Department of Mechanical Engineering, University of Bristol

[3]Institute of Sound and Vibration Research, University of Southampton

June 22, 2015

Outline

TE noise problems are important

Figure 1: Applications where TE noise is important

[1] [2] [3]

[1] Fig(a): sites.google.com/site/flightdeckathome/liveatc

[2] Fig(b): blog.journals.cambridge.org/2013/01/wind-turbine-syndrome-fact-or-fiction

[3] Fig(c): www.aliexpress.com/promotion/electronic_computer-fan-noise-promotion.html

TE noise problems are important

- TE noise of an approaching aircraft

(a) An approaching aircraft

Figure 1: Applications where TE noise is important

1 2 3

[1] Fig(a): sites.google.com/site/flightdeckathome/liveatc

[2] Fig(b): blog.journals.cambridge.org/2013/01/wind-turbine-syndrome-fact-or-fiction

[3] Fig(c): www.aliexpress.com/promotion/electronic_computer-fan-noise-promotion.html

TE noise problems are important

- TE noise of an approaching aircraft
- TE noise of wind turbines

(a) An approaching aircraft

(b) Wind turbines

Figure 1: Applications where TE noise is important

1 2 3

[1] Fig(a): sites.google.com/site/flightdeckathome/liveatc

[2] Fig(b): blog.journals.cambridge.org/2013/01/wind-turbine-syndrome-fact-or-fiction

[3] Fig(c): www.aliexpress.com/promotion/electronic_computer-fan-noise-promotion.html

TE noise problems are important

- TE noise of an approaching aircraft
- TE noise of wind turbines
- TE noise of rotating fans

(a) An approaching aircraft   (b) Wind turbines   (c) A rotating fan

Figure 1: Applications where TE noise is important

1 2 3

[1] Fig(a): sites.google.com/site/flightdeckathome/liveatc

[2] Fig(b): blog.journals.cambridge.org/2013/01/wind-turbine-syndrome-fact-or-fiction

[3] Fig(c): www.aliexpress.com/promotion/electronic_computer-fan-noise-promotion.html

Outline

TE noise generation

Focus on the turbulent-boundary-layer TE noise, which will be referred to as TE noise.

TE noise generation

Focus on the turbulent-boundary-layer TE noise, which will be referred to as TE noise.

When the turbulent boundary layer convects past the TE, the non-radiating pressure fluctuation is scattered into sound capable of propagating to the far-field.

Figure 2: TE noise generation by edge-scattering

TE noise reduction techniques

Figure 3: TE noise reduction techniques

4 5 6 7

[4] Fig(a): T.Geyer *et al* 2010

[5] Fig(b): Michaela Herr *et al* 2005

[6] Fig(c): Gruber's PhD thesis 2012

[7] Theory: (a) and (b) Jaworski and Peake 2013, Lorlna Ayton (c) Howe 1991

TE noise reduction techniques

- Porous airfoil

(a) Porous airfoil

Figure 3: TE noise reduction techniques

[4] [5] [6] [7]

[4] Fig(a): T.Geyer *et al* 2010

[5] Fig(b): Michaela Herr *et al* 2005

[6] Fig(c): Gruber's PhD thesis 2012

[7] Theory: (a) and (b) Jaworski and Peake 2013, Lorlna Ayton (c) Howe 1991

TE noise reduction techniques

- Porous airfoil
- Brush-type TE

(a) Porous airfoil (b) Brush-type TE

Figure 3: TE noise reduction techniques

[4] [5] [6] [7]

[4] Fig(a): T.Geyer *et al* 2010

[5] Fig(b): Michaela Herr *et al* 2005

[6] Fig(c): Gruber's PhD thesis 2012

[7] Theory: (a) and (b) Jaworski and Peake 2013, Lorlna Ayton (c) Howe 1991

TE noise reduction techniques

- Porous airfoil
- Brush-type TE
- Serrated TEs

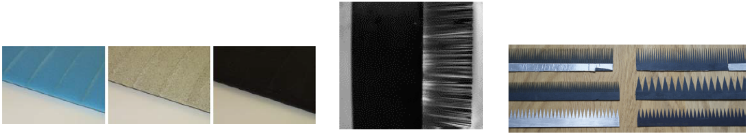

(a) Porous airfoil (b) Brush-type TE (c) Serrated TEs

Figure 3: TE noise reduction techniques

[4] [5] [6] [7]

[4] Fig(a): T.Geyer *et al* 2010

[5] Fig(b): Michaela Herr *et al* 2005

[6] Fig(c): Gruber's PhD thesis 2012

[7] Theory: (a) and (b) Jaworski and Peake 2013, Lorlna Ayton (c) Howe 1991

Howe's model

Howe's model significantly overpredictes the noise reduction capability of serrated TEs.

Figure 4: Comparison of experiment and Howe's model

8

[8] Fig4: Gruber's PhD thesis 2012

Howe's model

Howe's model significantly overpredictes the noise reduction capability of serrated TEs.

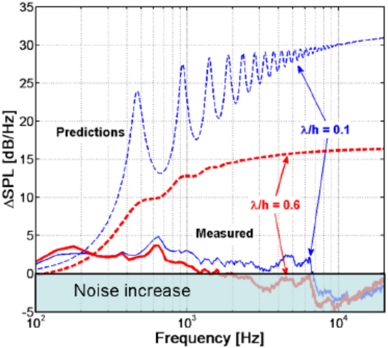

Figure 4: Comparison of experiment and Howe's model

8

[8] Fig4: Gruber's PhD thesis 2012

Outline

The mathematical model

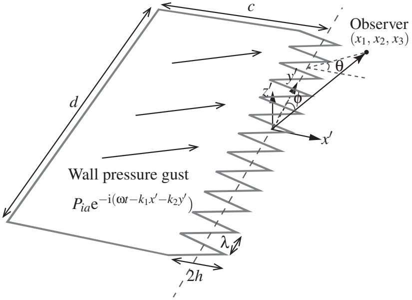

Figure 5: The schematic of a flat plate with a serrated TE

The following wave equation needs to be solved (Roger and Moreau 2013)

$$\left(\beta^2 + {H'}^2(y)\right)\frac{\partial^2 P}{\partial x^2} + \frac{\partial^2 P}{\partial y^2} + \frac{\partial^2 P}{\partial z^2} - 2H'(y)\frac{\partial^2 P}{\partial x \partial y} + \left(2iM_0 k - H''(y)\right)\frac{\partial P}{\partial x} + k^2 P = 0, \tag{1}$$

Fourier transformation

Making use of Fourier transformation

$$P(x, y, z) = \sum_{-\infty}^{\infty} P_n(x, z) e^{ik_{2n} y}, \tag{2}$$

where, $k_{2n} = k_2 + 2n\pi/\lambda$,

Fourier transformation

Making use of Fourier transformation

$$P(x,y,z) = \sum_{-\infty}^{\infty} P_n(x,z) e^{ik_{2n}y}, \tag{2}$$

where, $k_{2n} = k_2 + 2n\pi/\lambda$, the wave equation reduces to

$$\mathcal{D}\mathbf{P} = \mathbf{A}\mathbf{P} + \mathbf{B}\frac{\partial \mathbf{P}}{\partial x}, \tag{3}$$

where,

$$\mathcal{D} = \left\{ \left(\beta^2 + \sigma^2\right) \frac{\partial^2}{\partial x^2} + \frac{\partial^2}{\partial z^2} + 2ikM_0 \frac{\partial}{\partial x} \right\}. \tag{4}$$

The iterative-solving procedure

$\mathbf{P}^{(0)}$ is obtained by solving

$$\mathcal{D}\mathbf{P} = \mathbf{A}\mathbf{P}. \tag{5}$$

The iterative-solving procedure

$\mathbf{P}^{(0)}$ is obtained by solving

$$\mathcal{D}\mathbf{P} = \mathbf{A}\mathbf{P}. \tag{5}$$

Then $\mathbf{P}^{(1)}$ is evaluated by solving

$$\mathcal{D}\mathbf{P} = \mathbf{A}\mathbf{P} + \mathbf{B}\frac{\partial \mathbf{P}^{(0)}}{\partial x}. \tag{6}$$

The iterative-solving procedure

$\mathbf{P}^{(0)}$ is obtained by solving

$$\mathcal{D}\mathbf{P} = \mathbf{A}\mathbf{P}. \tag{5}$$

Then $\mathbf{P}^{(1)}$ is evaluated by solving

$$\mathcal{D}\mathbf{P} = \mathbf{A}\mathbf{P} + \mathbf{B}\frac{\partial \mathbf{P}^{(0)}}{\partial x}. \tag{6}$$

Continuing this process, $\mathbf{P}^{(2)}$ is found by solving

$$\mathcal{D}\mathbf{P} = \mathbf{A}\mathbf{P} + \mathbf{B}\frac{\partial \mathbf{P}^{(1)}}{\partial x}. \tag{7}$$

The iterative-solving procedure

$\mathbf{P}^{(0)}$ is obtained by solving

$$\mathcal{D}\mathbf{P} = \mathbf{A}\mathbf{P}. \tag{5}$$

Then $\mathbf{P}^{(1)}$ is evaluated by solving

$$\mathcal{D}\mathbf{P} = \mathbf{A}\mathbf{P} + \mathbf{B}\frac{\partial \mathbf{P}^{(0)}}{\partial x}. \tag{6}$$

Continuing this process, $\mathbf{P}^{(2)}$ is found by solving

$$\mathcal{D}\mathbf{P} = \mathbf{A}\mathbf{P} + \mathbf{B}\frac{\partial \mathbf{P}^{(1)}}{\partial x}. \tag{7}$$

A solution sequence

$$\mathbf{P}^{(0)}, \mathbf{P}^{(1)}, \mathbf{P}^{(2)}, \mathbf{P}^{(3)} \dots$$

Far-field sound

The far-field sound is obtained by evaluating the surface integral based on the theories of Kirchoff and Curle.

$$p_f(\mathbf{x}, \omega) = \frac{-i\omega x_3}{4\pi c_0 S_0^2} \iint_s \Delta P(x', y') e^{-ikR} \mathrm{d}\, x' \mathrm{d}\, y', \tag{8}$$

where $S_0^2 = x_1^2 + \beta^2(x_2^2 + x_3^2)$, and R takes the following form:

$$R = \frac{M_0(x_1 - x') - S_0}{\beta^2} + \frac{x_1 x' + x_2 y' \beta^2}{\beta^2 S_0}, \tag{9}$$

where, ΔP denotes the pressure jump across the flat plate.

Outline

FEM validation

For wide serrations

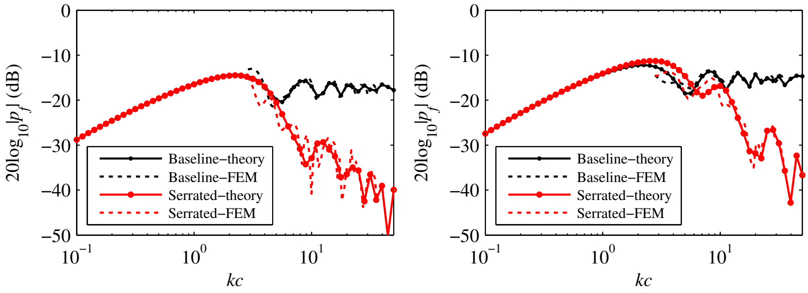

(a) $M_0 = 0.1$ (b) $M_0 = 0.2$

Figure 6: SPL at 90° above the trailing-edge in the mid-span plane with $x_3 = 1$ due to a wall pressure gust of frequency ω with $k_2 = 0$, parameters of the serrations are $\lambda/h = 6, h/c = 0.025$.

FEM validation cont.

For narrow serrations,

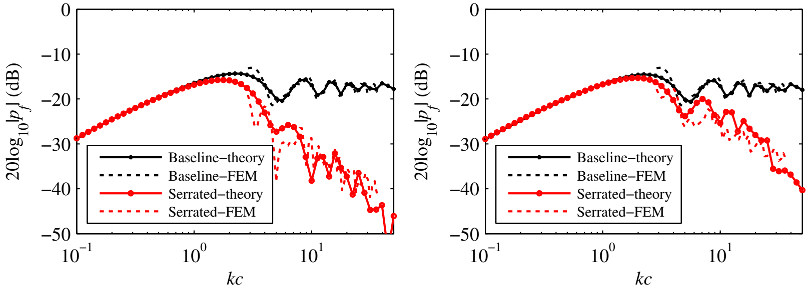

(a) $\lambda/h = 3$ (b) $\lambda/h = 1$

Figure 7: SPL at $90°$ above the trailing-edge in the mid-span plane with $x_3 = 1$ due to a wall pressure gust of frequency ω with $k_2 = 0$, parameters of the serrations are $h/c = 0.05$ with $M_0 = 0.1$.

Model results

For wide serrations,

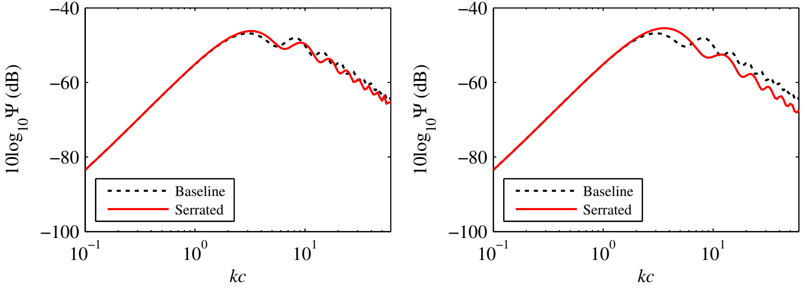

(a) $\lambda/h = 8$ (b) $\lambda/h = 4$

Figure 8: The normalized spectrum for straight and serrated trailing-edges, $h/c = 0.025, M_0 = 0.1$, the observer is at 90° above the trailing-edge in the mid-span plane with $x_3 = 1\lambda/h = 8$, $\lambda/h = 4$.

Model results cont.

For narrow serrations,

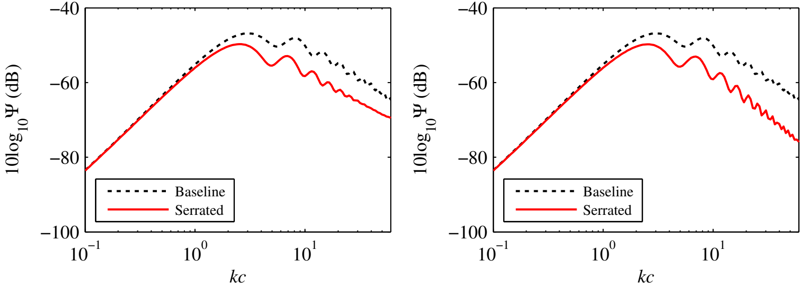

(a) $\lambda/h = 0.4$ (b) $\lambda/h = 0.2$

Figure 9: The normalized spectrum for straight and serrated trailing-edges, $h/c = 0.05, M_0 = 0.1$, the observer is at 90° above the trailing-edge in the mid-span plane with $x_3 = 1$.

Comparison with Howe's model

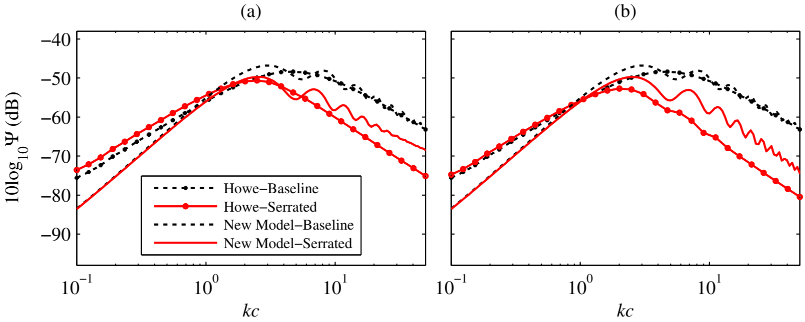

Figure 10: The normalized spectrum of Howe's model and the new model, $h/c = 0.05, M_0 = 0.1$, the observer is at 90° above the trailing-edge in the mid-span plane with $x_3 = 1$. (a)$\lambda/h = 0.4$, $h/c = 0.05$, $M_0 = 0.1$ (b) $\lambda/h = 0.2$, $h/c = 0.05$, $M_0 = 0.1$

Noise reduction mechanism

$$\sigma = 5$$

(a) $k\lambda = \pi/10$, (b) $k\lambda = \pi/5$, (c) $k\lambda = \pi/2$, (d) $k\lambda = \pi$

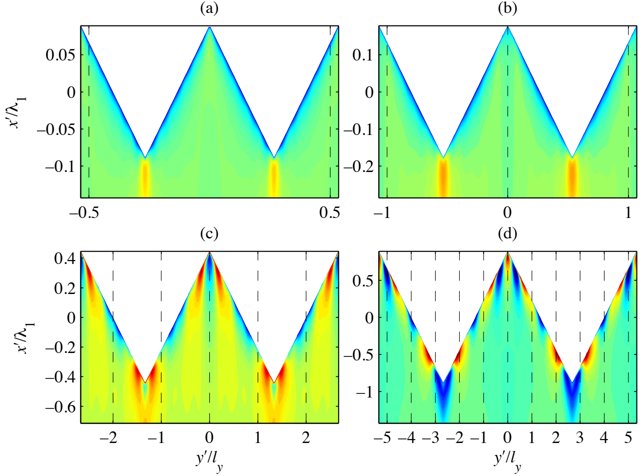

Outline

Conclusion

1. Compared to Howe's model, the presented model includes the convection effect of the mean flow, and can better agrees with experiments.
2. It is found that the destructive interference of the scattered pressure is the cause of sound reduction.
3. The approach used in this model can be used for other serrations. Future work on optimizing the serration profiles can be done.

Thank You!